ciated by an ArF excimer laser. The similarity of the absorption spectrum to that of diethylzinc and the expectation that a metallic atom (or at least a metallic ion) often results in the zinc case give us reason to expect a large quantum yield for beryllium, at least for some frequency range, in diethylberyllium photodissociation.

For a cross section of 0.18 Å^2 and a beam diameter of 0.1 mm, the 193-nm laser energy required for unit probability of absorbing a photon during one pulse is only 5 μJ (assuming the pulse length to be small compared to relevant diffusion times, which is easily the case for a typical pulse length of 20 ns). If the dye laser beam at 235 nm has a diameter of 0.5 mm, the diffusion time from the beam center for 250 torr of helium is 87 μs [assuming a diffusion constant of 1.8 cm^2/s, derived from magnesium and cadmium data (*15*)]. If the dye laser beam power is 5 mW, the Doppler broadening is 6.0 GHz (room temperature), and the collision broadening is 3.7 GHz [extracted from data for magnesium, calcium, and strontium in helium (*16*), with scaling as the 0.3 power of the temperature], then 870 photons will be emitted as the atom diffuses from the cell center. If the detection efficiency is 5% (light collection and quantum efficiency of the photomultiplier tube at 235 nm), 43 photons will be detected. With careful baffling and absorption of stray laser light, the primary source of background will be Rayleigh scattering from the helium gas in the focal volume. This Rayleigh yield will be 84 detected photons if the length of the imaged region along the beam is 2 mm. By looking at the number of counts during the 87-μs period after the 193-nm pulse, one can thus count bursts above background. A measurement could be completed in a few minutes.

The efficiency for detecting a beryllium atom formed at the center of the dye laser beam and within the imaging region of the phototube is approximately unity. However, the total efficiency is reduced by the ratio of the length of the imaged region to the length of the cell traversed by the photodissociation laser. A major experimental problem that will have to be resolved is balancing the efficiency of detecting a beryllium atom and the reduction of scattered light. If the entrance and exit windows were closed to the region that the phototube images, there would be scattered light produced as the dye laser beam passes through (in addition to Rayleigh-scattered light from the buffer gas). If these windows were far from the imaged region, there would be significant volumes inside the cell where the molecule would be dissociated but the beryllium atom would not be detected. If the windows were placed far away, thin plastic membranes (about 10 μg/cm^2) 4 mm apart enclosed the diethylberyllium molecules, and the imaged region were 2 mm long, as above, the total efficiency would be 50%. The number of atoms in the membranes (outside the focal volume) exposed to the laser beam would be less than the number of helium atoms in the focal volume, so Rayleigh scattering from the helium would remain the major source of background. Looking only at delayed photons when the dye laser is rapidly modulated on and off may help, but this would have to be done on a nanosecond time scale. An alternative would be to use two-photon rather than one-photon dissociation and to focus the dissociating laser into the imaged region.

REFERENCES AND NOTES

1. R. Davis, Jr., in *Neutrino '88: Proceedings of the Thirteenth International Conference on Neutrino Physics and Astrophysics*, J. Schneps *et al.*, Eds., Boston, MA, 5 to 11 June 1988 (World Scientific, Singapore, 1989), p. 518.
2. K. S. Hirata *et al.*, *Phys. Rev Lett.* **65**, 1297 (1990).
3. A. I. Abazov *et al.*, *ibid.* **67**, 3332 (1991).
4. J. N. Bahcall, *Phys. Lett.* **13**, 332 (1964); F. Reines and R. M. Woods, Jr., *Phys. Rev. Lett.* **14**, 20 (1965); J N. Bahcall, *ibid.* **23**, 251 (1969).
5. J. N. Bahcall and R. K. Ulrich, *Rev. Mod. Phys.* **60**, 297 (1988).
6. J. K. Rowley, in *Proceedings of the Informal Conference on the Status and Future of Solar Neutrino Research*, Brookhaven National Laboratory report no. 50879, G. Friedlander, Ed., Brookhaven National Laboratory, Upton, NY, 5 to 7 January 1978 (Brookhaven National Laboratory, Upton, NY, 1978) vol. 1, p. 265.
7. E. P. Veretenkin, V. N. Gavrin, E. A. Yanovich, *Sov. At. Energy* **58**, 82 (1985); V. N. Gavrin and E. A. Yanovich, *Bull. Acad. Sci. USSR Phys. Ser.* **51** (no. 6), 191 (1987)
8. S. L. Kaufman *et al.*, *Hyperfine Interact.* **4**, 921 (1978); C. L. Pan *et al.*, Opt. Lett. **5**, 459 (1980).
9. E. Borsella and R. Larciprete, *Appl. Surf. Sci.* **36**, 221 (1989).
10. CVD Inc., Woburn, MA.
11. Suprasil I was obtained from CVI Laser Corp., Albuquerque, NM.
12. MKS Instruments, Inc., Andover, MA.
13. Model 17D, Cary Inc., the spectrophotometers are now manufactured by Varian, Sunnyvale, CA.
14. Y Fujita, S. Fujii, T. Iuchi, *J. Vac. Sci. Technol.* **A7** (no. 2), 276 (1989).
15. K. M. Aref'ev, M. A. Guseva, B. M. Khomchenkov, *High Temp. (USSR)* **25** (no. 2), 174 (1987).
16. R G. Giles and E. L. Lewis, *J. Phys. B* **15**, 2871 (1982).

17. I am grateful to T. W. Newton for the use of the spectrophotometer. Funded by the U.S. Department of Energy.

6 January 1992; accepted 13 March 1992

Synthesis and Single-Crystal X-ray Structure of a Highly Symmetrical C_{60} Derivative, $C_{60}Br_{24}$

Fred N. Tebbe, Richard L. Harlow, D. Bruce Chase, David L. Thorn, G. Creston Campbell, Jr., Joseph C. Calabrese, Norman Herron, Robert J. Young, Jr., E. Wasserman

C_{60} and liquid bromine react to form $C_{60}Br_{24}$, a crystalline compound isolated as a bromine solvate, $C_{60}Br_{24}(Br_2)_x$. The x-ray crystal structure defines a new pattern of addition to the carbon skeleton that imparts a rare high symmetry. The parent C_{60} framework is recognizable in $C_{60}Br_{24}$, but sp^3 carbons at sites of bromination distort the surface, affecting conformations of all of the hexagonal and pentagonal rings. Twenty-four bromine atoms envelop the carbon core, shielding the 18 remaining double bonds from addition. At 150° to 200°C there is effectively quantitative reversion of $C_{60}Br_{24}$ to C_{60} and Br_2.

Early studies on fullerene carbon clusters point to an unusual chemical reactivity of this class of molecules. Of great interest are patterns that may develop on the surfaces of these polyhedra by repeated addition of atoms or more complex chemical groups. Although structures have been determined for compounds where C_{60} (*1*) is attached to as many as six metal complexes (*2*), structural information has not been available for derivatives with large numbers of addends.

We report the synthesis and structure of a new compound in which 24 bromine atoms bond to C_{60} (*3*). The product, $C_{60}Br_{24}$, displays T_h symmetry, only slightly reduced from the I_h symmetry of the parent molecule (Fig. 1). The pattern of the 24 bromines may be viewed as arising from 1,4-additions to fused pairs of six-membered rings with the closest Br,Br placement being 1,3 (*4*). Any further addition of Br is then unlikely because some Br atoms would necessarily be located on adjacent carbons.

When C_{60} and liquid bromine are combined at ambient temperatures, a solution is produced from which a yellowish-orange solid slowly precipitates (*6*). Although the solid is crystalline, the dimensions of the largest crystals are ~1 μm in size, much too small for a single-crystal x-ray structure determination. However, enough information could be obtained from infrared (IR) and Raman vibrational spectra to postulate a structure. When a crystal of sufficient size

Central Research and Development, E. I. du Pont de Nemours & Company, Inc., P.O. Box 80328, Wilmington, DE 19880–0328.

was grown, the x-ray study confirmed this structure and yielded details of the crystal and molecular form (Table 1).

The composition of the crystals determined by elemental analyses showed that 25 to 28 bromine atoms were present for each C_{60}, the number varying with the sample. Vibrational spectra indicated that the product was a single species of high symmetry and contained a center of symmetry. The highest symmetry available for a brominated fullerene, $C_{60}Br_n$, with n close to 25 to 28 is the cubic point group, T_h (7), having n equal to 24 or 30. A "classical" structure having a fullerene C_{60} framework, 24 equivalent bromines with single C–Br bonds, and T_h, symmetry is the $C_{60}Br_{24}$ structure shown in Fig. 1. This structure, supported by vibrational and x-ray data discussed below, has the additional feature that it admits a well-defined pattern of 72 C–C bonds and 18 C=C bonds. We also observed spectral bands that could be assigned to "free" Br_2, suggesting that the crystal composition and molecular structure could be reconciled as $C_{60}Br_{24}(Br_2)_{\sim 0.5-2}$.

Table 1. Fractional coordinates and isotropic (or equivalent) thermal parameters ($B_{iso/eq}$) with estimated standard deviations (in parentheses).

Atom	X	Y	Z	$B_{iso/eq}$
Br1	−0.0447 (1)	0.1490 (1)	0.33862 (3)	1.25 (4)*
Br2	−0.3764 (1)	0.0355 (1)	0.41932 (4)	1.19 (4)*
Br3	−0.1845 (1)	0.3224 (1)	0.49041 (4)	1.06 (4)*
Br4	0.1433 (1)	0.4306 (1)	0.40841 (4)	1.18 (4)*
Br5†	0.0000	0.0000	0.0510 (3)	6.9 (2)*
Br6'‡	0.0094 (33)	0.1044 (28)	0.0107 (11)	6.5 (2)
Br6"‡	0.0131 (17)	0.1629 (17)	0.0305 (6)	2.4 (3)
C1	−0.0287 (10)	0.1019 (10)	0.3951 (4)	0.8 (2)
C2	−0.1228 (10)	−0.0269 (10)	0.4028 (3)	0.7 (2)
C3	−0.2172 (10)	−0.0565 (10)	0.4269 (4)	0.8 (2)
C4	−0.2417 (10)	0.0300 (10)	0.4476 (4)	0.8 (2)
C5	−0.1320 (9)	0.1513 (10)	0.4500 (3)	0.6 (2)
C6	−0.0355 (10)	0.1853 (10)	0.4263 (3)	0.5 (2)
C7	−0.1238 (9)	0.2065 (10)	0.4909 (4)	0.6 (2)
C8	0.0006 (10)	0.2680 (10)	0.5078 (4)	0.8 (2)
C9	0.0973 (10)	0.3007 (10)	0.4840 (4)	0.8 (2)
C10	0.0886 (10)	0.2782 (10)	0.4390 (3)	0.6 (2)

*Refined with anisotropic thermal parameters. †Refined with an occupancy of 0.5. ‡Refined with an occupancy of 0.0833.

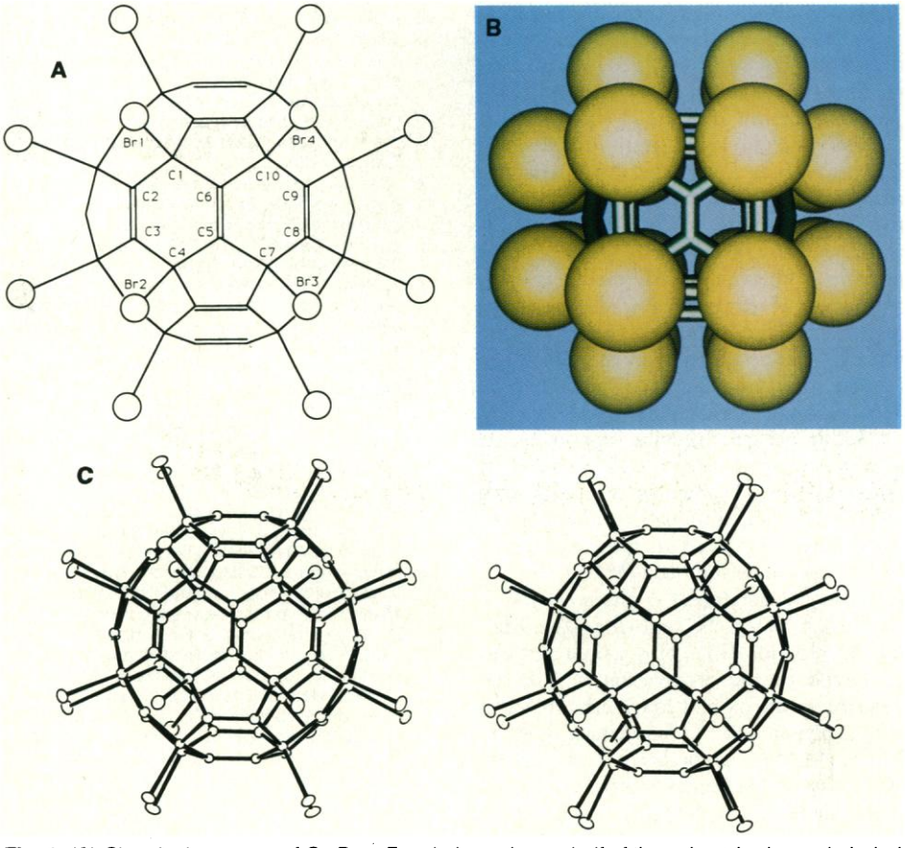

Fig. 1. (**A**) Chemical structure of $C_{60}Br_{24}$. For clarity, only one-half of the sphere is shown. Labeled atoms make up the crystallographic asymmetric unit. Unsaturated six-membered rings (for example, the ring defined by C1-C6) have bromines on C1 and C4 ("1,4-addition"). Saturated six-membered rings have bromines on alternate carbons ("1,3,5-addition"); "1,2-addition," not seen in the stable form of $C_{60}Br_{24}$ reported here, refers to addition at C5 and C6. (**B**) Color drawing of the $C_{60}Br_{24}$ molecule. With a radius of 1.85 Å, the Br atoms are seen to effectively cover the surface of the fullerene. (**C**) Stereodrawing of $C_{60}Br_{24}$ (50% ellipsoids).

The single-crystal x-ray study (8) showed that $C_{60}Br_{24}$ rigorously displays only crystallographic $\bar{3}$ symmetry, but the pattern of C–C and C=C bonds and the regular arrangement of Br atoms clearly place this molecule in the chemical point group T_h (Fig. 1). Average values for C–Br, C–C, and C=C bond distances are 1.993(6), 1.500(19), and 1.339(6) Å, respectively, with the estimated standard deviations (numbers in parentheses) based on divergence from the mean value; the individual values ranged from 1.985(12) to 2.000(11), 1.466(15) to 1.513(15), and 1.346(16) to 1.332(16) Å, respectively. The 24 carbon atoms that bond to bromines

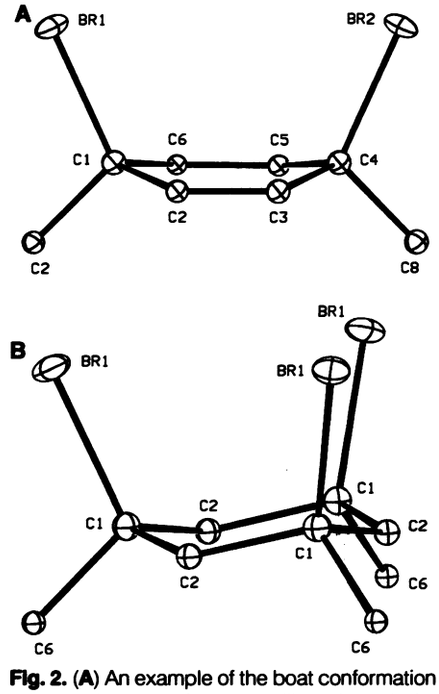

Fig. 2. (**A**) An example of the boat conformation adopted by one of the 1,4-dibrominated six-membered rings. (**B**) An example of the chair conformation adopted by one of the 1,3,5-tribrominated six-membered rings. Thermal ellipsoids are drawn at the 50% probability level.

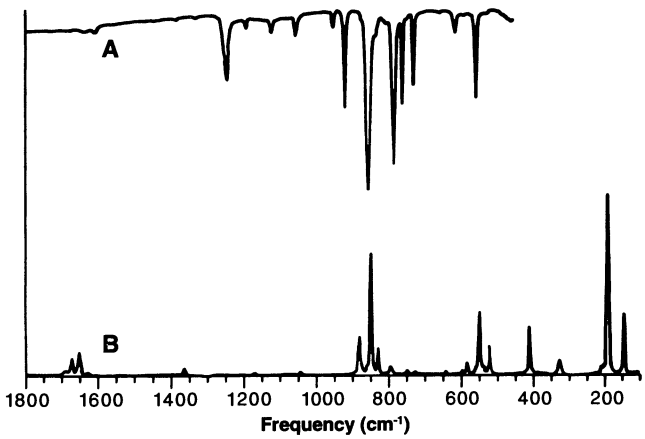

Fig. 3. (**A**) Infrared spectrum of $C_{60}Br_{24}(Br_2)_x$. (**B**) Raman spectrum.

adopt a tetrahedral geometry in which the average C–C–Br angle is 110.9(1.1)°. These 24 carbon atoms achieve tetrahedral geometry by protruding outward from the fullerene sphere and thereby create a rumpled surface. Bromines attached to carbon at the 1 and 4 positions cause 12 of the six-membered rings to adopt boat conformations; the remaining eight six-membered rings with bromines at the 1, 3, and 5 positions adopt chair conformations (Fig. 2) (9).

The crystal structure was complicated by the presence of additional electron density situated in the hollows of the ABCABC layers of this pseudo-cubic (face-centered-cubic), close-packed structure. Chemical analyses and spectroscopic data indicated that free Br_2 was present (see above); the extra peaks in the electron density map were assigned as interstitial Br_2 molecules. The positions and magnitudes of the peaks indicated that approximately one Br_2 molecule was present for every $C_{60}Br_{24}$ molecule. This Br_2 molecule, however, was found to be disordered over 14 sites distributed about a crystallographic $\bar{3}$ axis. Not only did this disorder make the refinement of the structure more difficult in general, but it also made an accurate determination of the actual amount of lattice Br_2 impractical. In the final cycles of the structural refinement, the total occupancy of these 14 sites was fixed at two bromine atoms in accord with the electron density. The chemical formula for the crystal used in this study was thus assigned as $C_{60}Br_{24} \cdot Br_2$. Lattice bromine was not evolved during heating overnight at 50°C, nor was its evolution detected by thermogravimetric analysis as a separate event, prior to complete decomposition at 150° to 200°C with formation of Br_2 and C_{60}.

From a normal mode analysis of this T_h structure (*10*), the C=C stretching modes span $2A_g + 2E_g + 3T_u + T_g$ irreducible representations. Only the five even (gerade) modes are Raman-active, whereas the three T_u modes are IR-active. These eight predicted modes were observed. Since $C_{60}Br_{24}$ has isolated C=C bonds, the observed frequencies should be higher than those in C_{60}, where unsaturation is delocalized. The highest IR frequencies observed for the parent C_{60} are at 1430 cm^{-1} (symmetry allowed) and 1534 cm^{-1} (symmetry forbidden) (*11*, *12*). In the IR spectrum of $C_{60}Br_{24}$ we observed three modes at 1688, 1641, and 1610 cm^{-1}. In the Raman spectrum, the highest frequency mode for C_{60} occurs at 1574 cm^{-1} (*12*, *13*). For $C_{60}Br_{24}$ we observed five modes at 1690, 1675, 1654, 1631, and 1607 cm^{-1} (Fig. 3).

Similarly, the C–Br stretch modes span $A_g + A_u + E_g + E_u + 3T_g + 3T_u$ irreducible representations and thus there should be five Raman-active modes and three IR-active modes involving C–Br stretching motions. We observed IR modes at 604, 546, and 527 cm^{-1}. The C–Br stretching modes are found in the region from 500 to 600 cm^{-1} for brominated alkenes (*14*). The Raman spectrum has modes at 585, 572, 536, 526, and 508 cm^{-1}.

Additional spectroscopic support for the highly symmetric structure is provided by the solid-state ^{13}C nuclear magnetic resonance spectrum, although quadrupolar effects are present even in spectra acquired with magic-angle spinning (MAS). An observed upfield multiplet is characteristic of coupling between ^{13}C and spin-3/2 nuclei, such as bromine (*15*). This assignment was confirmed by the observation of field-dependent splittings and linewidths in MAS spectra acquired at ^{13}C frequencies of 90.53 and 31.48 MHz. In both cases, the center of gravity of the signal intensity falls between about 30 and 40 ppm, a range which is reasonable for sp^3 carbons attached to bromine. A sharp peak at ~141 ppm was assigned to sp^2-hybridized carbons. Relative intensities of the olefinic and aliphatic regions were ~3:2, in agreement with the molecular structure of $C_{60}Br_{24}$.

Finally, we note that the remarkably high symmetries of C_{60} and certain polysubstituted derivatives may have manifestations on a macroscopic thermodynamic level. Although the reactions written below are only hypothetical, both the initial (Eq. 1) and the final brominations (Eq. 2) involve large changes in symmetry. In systems where symmetrical molecules rotate essentially freely in the classical limit, the molar entropy is less than it would be for related molecules having only mirror or trivial (C_1) symmetry. Thus in Eq. 1, the loss of C_{60} symmetry makes the process as written more favorable, and in Eq. 2 the gain of symmetry makes the process less favorable (*16*). The overall reaction leading to $C_{60}Br_{24}(Br_2)_x$ may be driven by product crystallization.

$$C_{60} + Br_2 = 1,4\text{-}Br_2C_{60} \quad (1)$$

$$C_{60}Br_{22} + Br_2 = C_{60}Br_{24} \quad (2)$$

REFERENCES AND NOTES

1. For papers on the discovery and synthesis of C_{60}, respectively, see, for example, H. W. Kroto, J. R. Heath, S. C. O'Brien, R. F. Curl, R. E. Smalley, *Nature* **318**, 162 (1985); W. Krätschmer, L. D. Lamb, K. Fostiropoulos, D. R. Huffman, *ibid.* **347**, 354 (1990).
2. P. J. Fagan, J. C. Calabrese, B. Malone, *J. Am. Chem. Soc.* **113**, 9408 (1991).
3. The isolation of this species was briefly noted prior to our determination of its structure [F. N. Tebbe *et al.*, *J. Am. Chem. Soc.* **113**, 9900 (1991)]. Evidence for addition of two to four bromines to C_{60} has been reported [G. A. Olah *et al.*, *ibid.*, p. 9385].
4. Although double bonds between six-membered rings have been identified as reactive sites for binding metal complexes [J. M. Hawkins, A. Meyer, T. A. Lewis, S. Loren, F. J. Hollander, *Science* **252**, 312 (1991), P. J. Fagan, J. C. Calabrese, B. Malone, *ibid.*, p. 1160; A. L. Balch, V. J. Catalano, J. W. Lee, *Inorg. Chem.* **30**, 3980 (1991)], addition of two bromine atoms across such a double bond (1,2-addition) would likely result in unfavorable eclipsed Br–Br interactions (*5*).
5. Although sites at which bromine and metals add are different, $C_{60}Br_{24}$ and the metal complex $C_{60}[Pt(PEt_3)_2]_6$ (Et, ethyl) (*2*) both have T_h symmetry. Up to five benzyl radicals add to C_{60} in 1,4-positions [P. J. Krusic, E. Wasserman, P. N. Keizer, J. R. Morton, K. F. Preston, *Science* **254**, 1183 (1991)]. A structure proposed for $C_{60}H_{36}$ [R. E. Haufler *et al.*, *J. Phys. Chem.* **94**, 8634 (1990)] is generated from the $C_{60}Br_{24}$ structure by addition of atoms at C5 and C6 sites (Fig. 1).
6. In a typical synthesis, a mixture of 0.10 g of C_{60} in 15 ml of liquid bromine was stirred under nitrogen at ambient temperature for 8 days. The solid product was isolated by filtration and dried overnight under vacuum (experimental analysis C, 25.3%; and Br, 75.5%). The yield was 0.34 g (86% based on the composition $C_{60}Br_{26.9}$). At 30°C, C_{60} in liquid bromine (0.13 ml/mg of C_{60}) was converted during 5.5 hours primarily to soluble brominated derivatives other than $C_{60}Br_{24}(Br_2)_x$. Conversion to $C_{60}Br_{24}(Br_2)_x$ was nearly complete in 2 to 3 days. A range of compositions has been obtained with C:Br ratios most often corresponding to $C_{60}Br_{27-28}$. $C_{60}Br_{24}(Br_2)_x$ has been exposed to air for days without change of the Raman spectrum, although the color darkens under ambient fluorescent light. The material lacks appreciable solubility in the reaction medium and in several common solvents.
7. The C_{60} fullerene framework lacks C_4 or S_4 axes, thus excluding point groups O_h, O, and T_d.

8. Sizable crystals of $C_{60}Br_{24} \cdot Br_2$ were grown directly from a reaction mixture consisting of C_{60} (35 mg) and Br_2 (5 ml) in a Teflon FEP tube tightly capped under nitrogen. Initially, the mixture was cooled from 70° to 65°C over 5 hours, and then to 55°C over 20 hours. The temperature was increased rapidly to 65°C and allowed to cool over 20 hours to 55°C. The latter routine was repeated, and finally the system was cooled from 65° to 25°C over 70 hours. An orange plate with dimensions of 0.16, 0.21, and 0.08 mm was mounted on a Syntex P3 diffractometer (graphite-monochromatized MoKα radiation, λ = 0.71069 Å) and cooled to −130°C. The rhombohedral unit cell parameters (in hexagonal form) determined from the Bragg angles of 50 computer-centered reflections are a = 12.874(2) and c = 32.659(6) Å. Six octants of intensity data were collected ($2\theta < 60°$), corrected for absorption (numerical integration: transmission factors ranged from 0.10 to 0.26), and finally averaged. The space group was assigned as $R\bar{3}$ (no. 148); the structure later confirmed the assignment. The structure was solved by direct methods and was refined by full-matrix least-squares techniques. The initial refinement of the $C_{60}Br_{24}$ molecule converged very quickly; a difference map at this point clearly indicated the presence of additional atoms that were assigned as Br_2 molecules of solvation (see text). Various disorder models were used to fit this extra density but the most successful included 14 sites distributed about the $\bar{3}$ symmetry axis located at the origin of the cell: two sites [Br(5)] were on the threefold axis itself, each of which were assigned an occupancy of 0.5; 12 other sites [Br6′ and Br6″] in general positions were assigned occupancies of 0.083. Attempts were made to refine the occupancies but the high correlation between the occupancies and the thermal parameters of the Br_2 atoms caused the least-squares refinement either to diverge or to converge to totally unacceptable values. The final refinement of 88 parameters (Br1 to Br5 with anisotropic thermal parameters; Br6′, Br6″, and C with isotropic thermal parameters; Table 1) in which 1229 unique reflections with $I > 2.5\sigma(I)$ were used converged at R = 0.039 and Rw = 0.038. The final difference map was featureless. The possibility of synthesizing more than one type of brominated species led to an examination of the reaction product by x-ray powder diffraction. The observed diffraction pattern was then compared with the "expected" pattern calculated from the single-crystal structure of $C_{60}Br_{24} \cdot Br_2$. The two patterns were found to be similar; the single crystal was clearly representative of the bulk product for these reaction conditions. Powder patterns of other samples have been observed to vary with synthesis conditions.
9. Carbons bonded to metal complexes and to the osmate group (*2, 4*) are also "pulled away" from the surface of the C_{60} cage.
10. Few molecules have T_h symmetry and the complete character table for this point group is sometimes omitted from textbooks. It is included in F. A. Cotton, *Chemical Applications of Group Theory* (Wiley, New York, ed. 2, 1971). (There is a misprint in the character of the inversion operation for the T_g and T_u representations.)
11. J. P. Hare *et al.*, *Chem. Commun.* **1991**, 412 (1991).
12. B. Chase, *J. Phys. Chem.*, in press.
13. D. S. Bethune *et al.*, *Chem. Phys. Lett.* **179**, 181 (1991).
14. D. Lin-Vien, N. Colthup, W. Fateley, J. Grasselli, *The Handbook of Infrared and Raman Characteristic Frequencies of Organic Molecules* (Academic Press, San Diego, CA, 1991), p. 31.
15. E. M. Menger and W. S. Veeman, *J. Magn. Reson.* **46**, 257 (1982); D. C. Apperley, B. Haiping, R. K. Harris, *Mol. Phys.* **68**, 1277 (1989).
16. The extent to which the formation of $C_{60}Br_{24}$ is disfavored depends on the number of isomers and symmetry of $C_{60}Br_{22}$.
17. We thank J. Sasson for his perspective on the chemical reactivity of Br_2; W. J. Marshall for skilled x-ray technical assistance; E. Pascher (Remagen) for elemental analyses; and D. A. Dixon, T. Fukunaga, J. Y. Becker, P. J. Krusic, and P. J. Fagan for helpful discussions. Contribution no. 6144.

24 January 1992; accepted 18 March 1992

Implication of GAP in Ras-Dependent Transactivation of a Polyoma Enhancer Sequence

Fabien Schweighoffer, Isabelle Barlat, Marie-Christine Chevallier-Multon, Bruno Tocque

Controversy exists as to whether the interaction of a guanosine triphosphatase activating protein (GAP) with Ras proteins functions both to initiate and to terminate Ras-dependent signaling events or only to terminate them. GAP-C, a carboxyl-terminal fragment of GAP that is sufficient to stimulate GTPase activity, inhibited the stimulation of transcription produced by some oncoproteins (v-Src, polyoma middle T, wild-type Ras, and oncogenic Ras) but not that produced by v-Mos. Wild-type GAP did not affect transcription induced by oncogenic Ras but reversed the inhibitory effect of GAP-C on transcription induced by oncogenic Ras. These results indicate that GAP is a negative regulator of wild-type Ras and elicits a downstream signal by interacting with Ras-GTP (guanosine triphosphate).

The function of GAP was investigated by studying its effect on the transcription from the polyoma virus–thymidine kinase (Py-TK) promoter, which is strongly activated by expression of Ras in Chinese hamster ovary (CHO) cells. Cells were cotransfected with a plasmid containing the chloramphenicol acetyl transferase (CAT) gene under the control of the Py-TK promoter (Py-TK-CAT), and expression vectors containing an oncogene and either the human GAP gene or the nucleotide sequence encoding its catalytic domain (amino acids 702 to 1044) under the control of the SV40 early promoter.

A common motif similar to the binding site for a protein (PEA1) that binds to the polyoma virus enhancer (GAGTTAGTCAC) is the target of action for oncoproteins such as v-Src, polyoma middle T, Ras, and v-Mos. In CHO cells all of these oncoproteins activated such an element containing four head-to-tail copies of the PEA1 motif from the polyoma virus enhancer (Fig. 1). Oncogenic Ras (Ha-Ras-Val^{12}) increased the rate of transcription from this element up to 15-fold. There is a good correlation between the capacities of various oncogenes to activate transcription from PEA1 and to transform cells (*1, 2*); furthermore, the loss of transactivation of the PEA1 motif correlates with phenotypic reversion (*3*). Oncogenic Ras also induces binding of nuclear proteins to a PEA1 motif

Rhône-Poulenc Rorer, Centre de Recherche de Vitry-Alfortville, 13 Quai Jules Guesde, B.P. 14, 94403 Vitry Sur Seine.

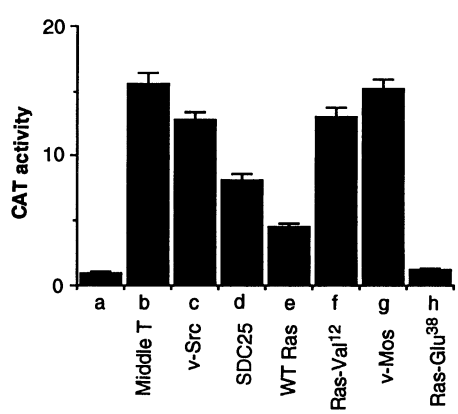

Fig. 1. Oncoprotein activation of an element from the polyoma virus enhancer. The cDNA sequences corresponding to the different transactivating proteins were inserted in an expression vector (SV2) downstream of the SV40 early promoter and enhancer (*1*). These plasmids were transfected into CHO cells with another vector containing CAT gene under the control of a Py-TK promoter (Py-TK-CAT). This synthetic promoter contains four head-to-tail copies of the PEA1 binding site of the polyoma enhancer upstream of the TK promoter. Lipospermine (Transfectam, IBF-SEPRACOR) was used as a transfecting agent. CHO cells (2×10^6) were transfected with Py-TK-CAT (0.5 μg) and 0.1 μg of the appropriate expression vector. Total DNA was adjusted to 5 μg with expression vector without insert. CAT activity was determined 48 hours after transfection and culture in Dulbecco's minimum essential medium (DMEM) supplemented with fetal calf serum (1%) as described (*32*). Data were recorded in arbitrary units; the basal signal due to activity of the reporter gene alone was assigned a value of 1. Columns a through h represent CAT activity in cells transfected with: (a) Py-TK-CAT alone, (b) sequences encoding polyoma middle T, (c) v-Src, (d) SDC25-C (*11*), (e) wild-type Ha-Ras, (f) Ha-Ras-Val^{12}, (g) v-Mos, or (h) Ha-Ras-Val^{12} Glu^{38}. The data are means of three independent experiments normalized to the CAT activity generated in the presence of the reporter gene alone.